

PAPER • OPEN ACCESS

## Power flow calculation method for DC distribution system with voltage source converter operation mode consideration

To cite this article: Shixiong Fan *et al* 2019 *IOP Conf. Ser.: Earth Environ. Sci.* **227** 032046

View the [article online](#) for updates and enhancements.

# Power flow calculation method for DC distribution system with voltage source converter operation mode consideration

Shixiong Fan<sup>1,4</sup>, Xingwei Liu<sup>1</sup>, Yanhong Yang<sup>2</sup>, Zechen Wei<sup>1</sup>, Yunxing Gao<sup>3</sup> and Wei Pei<sup>2</sup>

<sup>1</sup> China Electric Power Research Institute, Beijing 100192, China;

<sup>2</sup> Institute of Electrical Engineering, Chinese Academy of Science, Beijing 100190, China;

<sup>3</sup> State Grid Tai'an Power Supply Company, Shandong 271000, China.

<sup>4</sup> Email: fanshixiong@epri.sgcc.com.cn

**Abstract.** This paper focuses on the power flow calculation method for DC distribution system with voltage source converter operation mode consideration. To accurately calculating the dc power flow, the master-slave and droop control mode of VSC converter station is used. The structure and mathematical model of VSC converter are discussed. When performing DC power flow calculation, the converter station is equivalent to P node/Slack node/D node according to different control modes of the converter station. And the non-linear DC network equations is solved with the Newton-Raphson (NR) method. A study case which is based on 11 nodes DC distribution system is used to carry out the DC power flow method, and simulation results show that the proposed model and method are effective.

## 1. Introduction

In recent years, using DC power for electrical distribution is getting more and more attention[1]. The power generation side is now witnessing a strong push towards renewable energy sources (RES), and RES is DC power normally [2-3]. Solar Photovoltaics (PV) naturally produce DC power, and different windfarms also produce DC power as an intermediate stage before converting to frequency AC. On the residential and commercial energy utilization side, the modern electronic loads are hungry for DC power [4-5]. Personal computers, laptops, LCD displays etc. use DC power and resort to an AC/DC conversion for being plugged into the current power system. Lighting, which is another big consumer of energy is also evolving as a consumer of DC energy with the Light Emitting Diodes (LED) based lighting for homes and offices. And some new types of DC loads such as data centers, electrical vehicles, and communication centers have widely appeared in recent years. According to nowadays development trends, these DC power sources and loads will have deep influence on future city power distribution systems. Also the DC grid is a suitable solution to manage clean energy resources [6], which is a topic with growing interest in the research community.

The DC power system normally has this structure, shown in Figure 1: DC bus act as connection point, and DC lines connect to DC buses to form a DC network. VSC stations connect to DC buses injecting power from ac power system. Such DC grid structure can simulate a variety of DC power grid topologies. Furthermore, it is extensible in the future if there are DC generators and DC loads which can be directly connected to DC buses.



The current work is related to the design, control, operation and efficiency of DC distribution networks. Paper [7] gives a review of the recent researches on design, control and analysis of DC distribution systems, and some advantages of DC distribution technology are also pointed out. The traditional shortcomings of DC system such as voltage transformation are overcome by advanced power electronics technology. The DC micro grid zones may be more and larger which can be treated as a complete DC distribution system, and the DC power technology provides a new way to solve the problem of RES. Paper [8] provides a design paradigm for performance optimization of DC distribution systems with lots of power electronics devices.

For the planning and operation of DC grid systems, it is required to perform a power flow analysis, which enables to calculate the voltage, power and the energy losses of different technical and operative aspects of the grid. The classical power flow equations and models are based on the realistic assumption that the dc grid has well defined operative conditions in terms of quality service and electrical connections [9]. In paper [10], a steady-state multi-terminal DC model for power flow programs has been developed which allows to include converter limits as well as different converter topologies. The authors of paper [11,12] present adaptations of classical methods such as Newton–Raphson or Gauss–Seidel to solve DC power flow problem. In paper [13], a linear power flow formulation for low-voltage DC power grids is discussed. The voltage droop control mode and power flow analysis are studied in paper [14,15]. The bus types of DC power system is related to the system operation mode, which need to be reconsidered carefully to adapt to the future DC power system development and construct. However, few of these studies consider the coupling relationship between the VSC operation mode and system power flow. Considering the aforementioned facts and problems, this paper focuses on the power flow calculation method for DC distribution system with VSC converter operation mode consideration.

Therefore, this paper in Section 2, the structure and mathematical model of VSC will be introduced. After that, the master-slave and droop control mode of VSC converter station will be given in Section 3. The DC power flow calculation method will be discussed in Section 4. Section 5 will be devoted to the case study and discussions. Finally, conclusions will be drawn in Section 6.

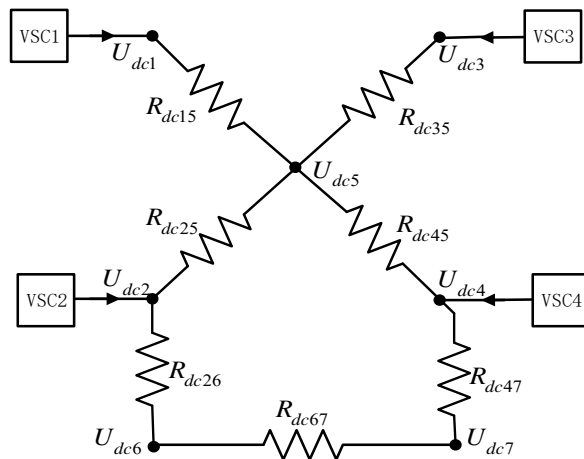


**Figure 1.** DC distribution system with voltage source converter (VSC).

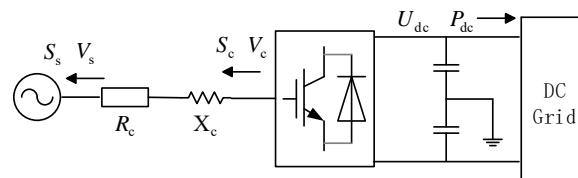


**Figure 2.** Voltage source converter (VSC) structure.

## 2. Mathematical model of VSC

In general format, the structure of VSC converter is shown in Figure 2. Each converter is connected to the AC grid and to the DC grid. The AC side is modelled by a voltage source coupled to the AC bus through a phase reactor. The DC side of the converter is modelled by a power injection into the DC grid.

AC grid point power equation:

$$\begin{cases} P_s = \frac{V_c V_s \cos(\delta_s - \delta_c + \delta_z)}{|Z_c|} - \frac{V_s^2}{|Z_c|} \cos \delta_z \\ Q_s = \frac{V_c V_s \sin(\delta_s - \delta_c + \delta_z)}{|Z_c|} - \frac{V_s^2}{|Z_c|} \sin \delta_z \end{cases} \quad (1)$$

Modulated point power equation:

$$\begin{cases} P_c = V_c^2 G_c - V_c V_s [G_c \cos(\delta_s - \delta_c) - B_c \sin(\delta_s - \delta_c)] \\ Q_c = -V_c^2 B_c + V_c V_s [G_c \sin(\delta_s - \delta_c) + B_c \cos(\delta_s - \delta_c)] \end{cases} \quad (2)$$

Where,  $Z_c$  is the phase reactor;  $G_c$  is the reactor conductance;  $B_c$  is the reactor susceptance;  $\delta_z$  is the reactor impedance angle; V, P, Q,  $\delta$  are on behalf of voltage, active power, reactive power and phase angle respectively; subscript s and c are on behalf of AC grid point and modulated point.

Here, the VSC converter station power loss is using a generalized loss formula with quadratic curve fitting of the converter current, which is given by:

$$P_{loss} = a + bI_c + cP_c^2 \quad (3)$$

Where, the converter current is given by:

$$I_c = \sqrt{P_c^2 + Q_c^2} / V_c \quad (4)$$

Figure 3 shows the VSC's operating point where operate in region I. The two axes in Figure 3 are the active P and reactive power Q. Positive values represent the VSC providing power and negative values represent the VSC absorbing power. The circles represent the rating capacity (i.e. maximum apparent power) of the VSC. The power provided by the VSC cannot exceed its rating capacity as equation (5).

$$\sqrt{P_1^2 + Q_1^2} \leq S_{max} \quad (5)$$

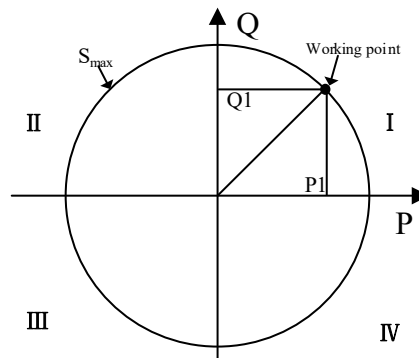


**Figure 3.** Active and reactive power operating point of VSC.

### 3. VSC station control mode

Since the VSC converter can realize independent control of active and reactive power, the VSC converter can control DC voltage or DC power of a DC side state variable, and can also control AC side voltage or AC side reactive power. So in the power flow calculation, different settings and node equivalents are required depending on the control mode of the VSC converter station.

### 3.1. Master-slave control mode

When operating in the master-slave control mode, the converter station with a larger capacity is generally used as the main converter station, and the other converter stations are used as the slave converter station. The main control objective of the main converter station is to maintain a stable DC bus voltage, also commonly referred to as a voltage station. The slave converter station is typically operated in accordance with a given active and reactive power, also known as a power station. In order to ensure the safe and stable operation of the system, the capacity of the main converter station is generally greater than the sum of other converter stations, and a certain margin is reserved, or the standby station is used to ensure the system reliability.

For the voltage converter station, it is responsible for controlling the DC bus voltage and balancing the active power in the network. When calculating the power flow, it is seen as the balance or slack node (U node), the initial value of the power is given as  $P_{dc0}$ , and the voltage converter station node generally has only one. If the voltage station fails, the standby station will switch from power control mode to DC bus voltage control mode.

For a power converter station, when performing DC power flow calculation, it is equivalent to a power node (P node), and the power injected into the DC system can be calculated by:

$$P_{dc} = P_c - P_{loss} \quad (6)$$

### 3.2. Droop control mode

The droop control means that each converter station realizes power sharing according to the DC power-voltage ramp to ensure the DC voltage is stable. In the DC system, the converter station can adjust the DC power setting value according to the measured value of the DC voltage to meet the DC power demand of the DC distribution network, and this adjustment method can be expressed by a curve of DC voltage  $U_{dc}$  and power  $P_{dc}$ , as shown in Figure 4.

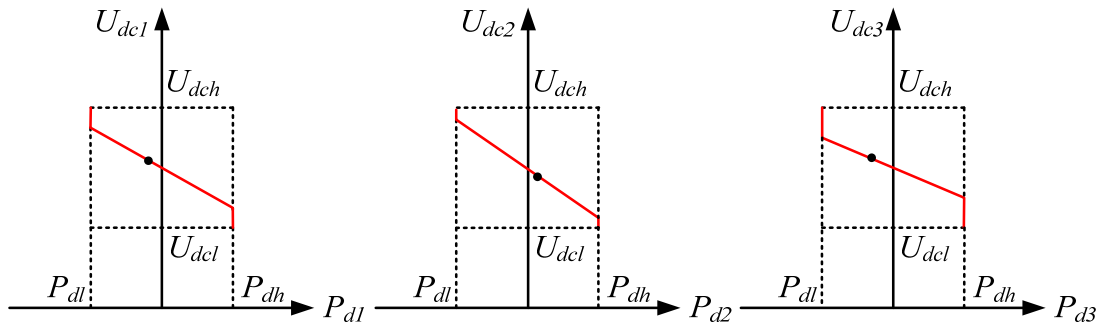


**Figure 4.** Operating point of droop control mode.

Using the P-V droop control method, the droop coefficient can be selected according to the following formula:

$$k_p = \frac{U_{dc}^{ref} - U_{dc}^{max}}{P_{dc}^{ref} - P_{dc}^{max}} \quad (7)$$

Where:  $k_p$  indicates the droop coefficient,  $U_{dc}^{ref}$  and  $U_{dc}^{max}$  represent the DC voltage reference value and maximum value respectively,  $P_{dc}^{ref}$  and  $P_{dc}^{max}$  represent the active power reference value and maximum value respectively.

The droop coefficient  $k_p$  determines how much unbalanced active power is distributed to each converter station in the DC network. If each converter station uses the same size  $k_p$ , the unbalanced power will be equally distributed to each converter station; at the same time, larger  $k_p$  means that less unbalanced power will be shared, and smaller  $k_p$  means more unbalanced power is shared.

When calculating the DC power flow, the converter station of the droop control mode is equivalent to the droop node (D node), and the relationship between voltage, power and droop coefficient is as follows:

$$U_{dc} = U_{dc}^{ref} + k_p (P_{dc} - P_{dc}^{ref}) \quad (8)$$

$$k_{pi} R_i = k_{pj} R_j \quad (9)$$

Where  $k_{pi}$  and  $k_{pj}$  are the droop coefficient of the converter stations  $i, j$ ;  $R_i$  and  $R_j$  are the capacity of the converter stations  $i, j$ .

#### 4. DC power flow calculation algorithm

When performing DC power flow calculation, the converter station is equivalent to P node/Slack node/D node according to different control modes of the converter station.

The current injected at a DC node  $i$  can be written as the current flowing to the other  $n-1$  nodes in the network:

$$I_{dci} = \sum_{\substack{j=1 \\ j \neq i}}^n Y_{dcij} \cdot (U_{dci} - U_{dcj}) \quad (10)$$

Combining all currents injected in an  $n$  bus DC network, the matrix form is given by:

$$I_{dc} = Y_{dc} U_{dc} \quad (11)$$

For a bipolar DC grid, the active power injected in node  $i$  can be written as

$$P_{dci} = 2U_{dci} I_{dci} \quad (12)$$

The current injections are not known prior to the power flow solution for the DC grid, whereas the active power injections are known for all buses except for the DC slack buses. Combining (10) and (12), we can get the system of nonlinear equations as following:

$$P_{dci} = 2U_{dci} \sum_{\substack{j=1 \\ j \neq i}}^n Y_{dcij} \cdot (U_{dci} - U_{dcj}) \quad (13)$$

In this paper, the non-linear DC network equations is solved with the Newton-Raphson (NR) method [10], the NR equation is given by:

$$\left( U_{dc} \frac{\partial P_{dc}}{\partial U_{dc}} \right)^{(j)} \cdot \frac{\Delta U_{dc}^{(j)}}{U_{dc}} = \Delta P_{dc}^{(j)} \quad (14)$$

In which, the mismatch power  $\Delta P_{dc}^{(j)}$  is given by each type of node:

$$\Delta P_{dc}^{(j)} = \begin{cases} P_{dc0i} - P_{dc0i}(U_{dc}^{(j)}) & \text{U node} \\ P_{dci} - P_{dci}(U_{dc}^{(j)}) & \text{D node} \\ -P_{dci}(U_{dc}^{(j)}) & \text{P node} \end{cases} \quad (15)$$

Where, superscripts (j) is referring to the NR iteration.

The terms for the Jacobian matrix calculation are given by:

$$\left( U_{dcj} \frac{\partial P_{dcj}}{\partial U_{dcj}} \right)^{(j)} = -2 \cdot U_{dci}^{(j)} Y_{dcij} U_{dcj}^{(j)} \quad (16)$$

$$\left( U_{dci} \frac{\partial P_{dci}}{\partial U_{dci}} \right)^{(j)} = P_{dci}^{(j)} + 2 \cdot U_{dci}^{(j)^2} \sum_{\substack{j=1 \\ j \neq i}}^n Y_{dcij} \quad (17)$$

The solution flow diagram of DC power flow is shown in Figure 5.

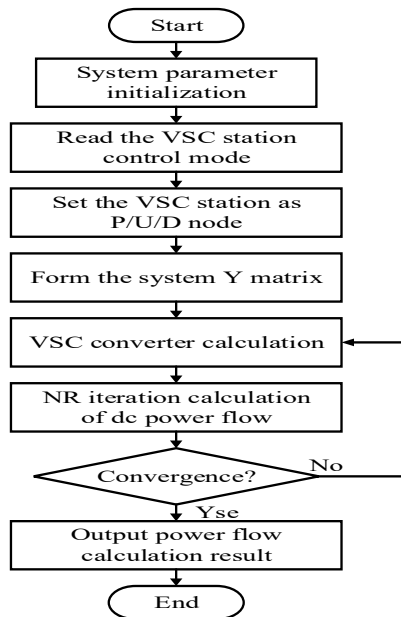


**Figure 5.** Solution flow diagram of DC power flow.

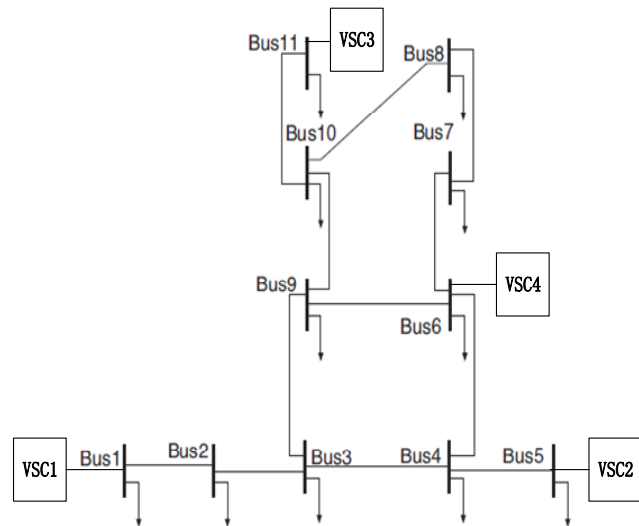


**Figure 6.** Simulation system configuration.

## 5. Study case simulation

**Table 1.** Resistances of test system.

	From bus	To bus	Resistance(Ω)
Line1	1	2	3.3
Line2	2	3	4.2
Line3	3	4	2.8
Line4	3	4	5.9
Line5	4	5	3.9
Line6	4	6	4.1
Line7	6	7	2.2
Line8	6	9	1.8
Line9	7	8	4.5
Line10	8	10	6.3
Line11	9	10	3.6
Line12	10	11	2.1

**Table 2.** Loads of test system.

bus	1	2	3	4	5	6
Load(kW)	100	-	190	-	-	130
		120		250	170	
bus	7	8	9	10	11	-
Load(kW)	220	-	240	-	130	-
		150		100		

**Table 3.** VSC convertor results of mode 1.

VSC	Mode	Voltage(p.u.)	Power(kW)
1	DC voltage control	0.9995	-384.6
2	Power control	1.0004	320.0
3	Power control	1.0002	180.0
4	Power control	0.9996	-350.0

**Table 4.** Power flow results of mode 1

Node	Voltage(p.u.)	Line	Power injected at "from " bus end(kW)
1	1	1	283.3
2	0.9953	2	402.0
3	0.9868	3	85.3
4	0.9856	4	123.3
5	0.9826	5	151.7
6	0.9818	6	183.4
7	0.9816	7	17.4
8	0.9863	8	-145.9
9	0.9832	9	-202.6
10	0.9880	10	-53.5
11	0.9903	11	-263.3
		12	-218.2

**Table 5.** VSC convertor results of mode 2

VSC	Mode	Voltage(p.u.)	Power(kW)
1	Droop control	0.9998	-196.8
2	Droop control	1.0003	239.6
3	Droop control	1.0001	78.7
4	Droop control	0.9996	-350.9

**Table 6.** Power flow results of mode 2

Node	Voltage(p.u.)	Line	Power injected at "from " bus end(kW)
1	1.0073	1	95.6
2	1.0057	2	215.4
3	1.0012	3	-33.6
4	1.0017	4	58.1
5	1.0003	5	70.9
6	0.9987	6	145.4
7	0.9985	7	23.4
8	1.0029	8	-88.2
9	0.9995	9	-196.6
10	1.0044	10	-47.5
11	1.0067	11	-270.3
		12	-219.1

The previously discussed method was applied on the 11 node and 4 VSC converter test system to verify its validity. The configuration of the studied system is shown in Figure 6.

The parameters of the studied system is shown in Table 1 and Table 2.

The DC power flow calculation results are below:

(1) Master-slave control mode

The VSC convertor results of DC power flow is shown in Table 3. The nodal voltage and power in each branch of master-slave control mode DC power flow is shown in Table 4.

(2) Droop control mode

The VSC convertor results of DC power flow is shown in Table 5. The nodal voltage and power in each branch of droop control mode DC power flow is shown in Table 6.

It can be seen that the power flow distribution of the system is different under the two control modes. For the case in this paper, the voltage of each node under the master-slave control is less than or equal to 1p.u., while the voltage of each node under the droop control fluctuates up and down at 1p.u. The power flow direction of branch in the two modes is basically the same, but the power distribution of each branch of the system under the droop control is more uniform than that under the master-slave control.

## 6. Conclusions

This paper presented a power flow calculation method for DC distribution system with voltage source converter operation mode consideration to improve calculation accuracy. After discussing the structures and mathematical model of VSC converter, the master-slave and droop control mode of VSC converter station is proposed. Then, according to different control modes of the converter station,



the converter station is equivalent to P node/Slack node/D node when calculating the DC power flow. The simulation results show that the proposed model and method are accurate and effective.

The proposed power flow analysis technique can be used for power losses minimization, economic power dispatch or other optimization problem via master-slave optimization structures. This method can be also used for distributed control and voltage regulation problem. The future work related to the efficiency and energy-savings of DC power distribution may be based on the methods presented in this paper.

### Acknowledgement

This work was supported in part by the National Key Research and Development Program of China under Grant (2017YFB0903300) and in part by the Science and Technology Research Foundation of SGCC (No. DZ71-17-030).

### References

- [1] Nordman B, Christensen K 2016 DC local power distribution: technology, deployment, and pathways to success[J] *IEEE Electrification Magazine* **4(2)** 29-36
- [2] Siddique H A B, De Doncker R W 2018 Evaluation of DC Collector-Grid Configurations for Large Photovoltaic Parks[J] *IEEE Transactions on Power Delivery* **33(1)** 311-320
- [3] Chuangpishit S, Tabesh A, Moradi-Shahrbabak Z, et al. 2014 Topology design for collector systems of offshore wind farms with pure DC power systems[J] *IEEE Transactions on Industrial Electronics* **61(1)** 320-328
- [4] Dragicevic T, Vasquez J C, Guerrero J M, et al. Advanced LVDC Electrical Power Architectures and Microgrids: A step toward a new generation of power distribution networks[J] *2014 IEEE Electrification Magazine* **2(1)** 54-65
- [5] AlLee G, Tschudi W 2012 Edison redux: 380 Vdc brings reliability and efficiency to sustainable data centers[J] *IEEE Power and Energy Magazine* **10(6)** 50-59
- [6] Elsayed A T, Mohamed A A, Mohammed O A 2015 DC microgrids and distribution systems: An overview[J] *Electric Power Systems Research* **119** 407-417
- [7] Blaabjerg F, Dragicevic T, Doolla S, et al. 2017 Recent Advances in Control, Analysis and Design of DC Distribution Systems and Microgrids[J]
- [8] Suryanarayana H, Sudhoff S D 2017 Design paradigm for power electronics-based DC distribution systems[J] *IEEE Journal of Emerging and Selected Topics in Power Electronics* **5(1)** 51-63
- [9] Garces A 2017 Uniqueness of the power flow solutions in low voltage direct current grids[J] *Electric Power Systems Research* **151** 149-153
- [10] Beerten J, Cole S, Belmans R 2012 Generalized steady-state VSC MTDC model for sequential AC/DC power flow algorithms[J] *IEEE Transactions on Power Systems* **27(2)** 821-829
- [11] Maknouninejad A, Qu Z, Lewis F L, et al. 2014 Optimal, nonlinear, and distributed designs of droop controls for DC microgrids[J] *IEEE Transactions on Smart Grid* **5(5)** 2508-2516
- [12] Ma J, Yuan L, Zhao Z, et al. 2017 Transmission loss optimization-based optimal power flow strategy by hierarchical control for DC microgrids[J] *IEEE Transactions on Power Electronics* **32(3)** 1952-1963
- [13] Montoya OD, Grisales-Noreña LF, González-Montoya D, et al 2018 Linear power flow formulation for low-voltage DC power grids[J] *Electric Power Systems Research* **163** 375-381
- [14] Rouzbehi K, Miranian A, Luna A, et al. 2014 DC voltage control and power sharing in multiterminal DC grids based on optimal DC power flow and voltage-droop strategy[J] *IEEE Journal of Emerging and selected topics in power Electronics* **2(4)** 1171-1180
- [15] Li C, Chaudhary S K, Savaghebi M, et al. 2017 Power flow analysis for low-voltage AC and DC microgrids considering droop control and virtual impedance[J] *IEEE Transactions on Smart Grid* **8(6)** 2754-2764